Fibers and Polymers 2020, Vol.21, No.12, 2842-2847
DOI 10.1007/s12221-020-9976-7

ISSN 1229-9197 (print version)
ISSN 1875-0052 (electronic version)

Improved Dyeing of Meta-aramid Based on Particle Flow Dyeing Mechanism Using Hot-pressing Dyeing Method

Xin Chen[1,3†], Dan Sheng[2,3†], Honghui Xia[4], Weilin Xu[2,3], Bo Deng[3]*, and Genyang Cao[3]*

[1]*Science and Technology Institute, Wuhan Textile University, Wuhan, Hubei 430200, China*
[2]*School of Textile and Clothing, Jiangnan University, Wuxi, Jiangsu 214000, China*
[3]*State Key Laboratory of New Textile Materials and Advanced Processing Technologies, Wuhan Textile University, Wuhan, Hubei 430200, China*
[4]*School of Textile, Wuhan Textile University, Wuhan, Hubei 430200, China*
(Received October 1, 2019; Revised March 18, 2020; Accepted March 28, 2020)

Abstract: In this study, a combined dyeing method by integrating the advantages of both carrier dyeing and hot-pressing dyeing was utilized for the dyeing of meta-aramid. A rapid dyeing with increased mechanical properties of the fibers was achieved for the meta-aramid fiber. A so-called particle flow mechanism involving both N,N-dimethylacetamide (DMAc) and dye molecules was proposed to explain the accelerating effect of this unique dyeing method. The mechanical properties and thermodynamic stability of the fiber after hot-pressing were both increased. XRD results showed increased corresponding fiber crystallinity. TEM showed that the disperse dyes were well dispersed in DMAc. Cross-sectional optical photographs of dyed fibers revealed that the dyes were successfully carried into the interior of the fiber under the synergic effect of temperature and pressure. Combined with hot-pressing dyeing, the dyeing cycle for the meta-aramid could be greatly shortened and the amounts of dyes and carriers could be significantly reduced.

Keywords: Meta-aramid, Hot-pressing dyeing, N,N-Dimethylacetamide, Particle flow dyeing

Introduction

Meta-aramid is a technologically advanced fiber with an excellent comprehensive performance [1,2]. It is widely used in special fields such as defense, aerospace, and renewable energy because of its high resistance to acid and alkali, corrosion, high temperature, and excellent flame retardant performance [3-7]. Meanwhile, extremely specific requirements for both the color and the properties of the dyed meta-aramid are necessary for these applications [8]. However, because of the dye-inert structure of meta-aramid, strong intermolecular hydrogen bonding force, and its high glass transition temperature, meta-aramid is difficult to be dyed [9-13].

Currently, the main dyeing methods for meta-aramid are stock-dyeing and post-dyeing [14]. The stock-dyeing method refers to adding a coloring agent before the spinning of the chemical fiber, and then the colored fiber could be directly obtained after the spinning process. This is a high-tech textile dyeing and finishing technology [15]. Stock-dyeing normally provides high dyeing uniformity and fastness, but it has certain limitations such as dull color and hardness in the controlling of the dyeing process [16]. The post-dyeing method is more suitable for mass production by providing both rich colors and controllable process. The carrier dyeing is a widely used technique belong to the post-dyeing method. In this method, the carrier can enter the fiber, destroy the hydrogen bond between fiber macromolecules, and increase the inter-fiber distance. Thus the fiber swells in the carrier and results in reduced structural density and enlarged surface area [13,17-19]. Finally, the dye could be more easily carried into the interior of the fiber and results in better dyeing effect. DMAc was previously reported to be used for the dyeing pretreatment of meta-aramid, or as a carrier during the dyeing process. It significantly improves the dyeing effect of meta-aramid while inevitably causes a decreased mechanical strength [20]. And also, a dyeing bath ratio up to 1:140 and a dyeing time up to 90 min of this method meant high pollution and time-consuming. Our dyeing technology uses a bath ratio of only 1:2 and dyeing time of only 10 min, which can reduce both the environmental pollution and energy consumption significantly.

Traditional hot melt dyeing [21,22] requires two steps: drying and curing at high temperature for around 10-30 min, whereas only one step is required for our technology to reduce the dyeing time to 10 min.

This paper reported a combined dyeing method by integrating the advantages of both carrier dyeing and hot-pressing dyeing. Meanwhile, a particle flow dyeing mechanism was proposed to explain the accelerated dyeing effect of hot-pressing dyeing. Formed particle flow consisting of both solvent and dye under high temperature and pressure implemented the rapid dyeing of meta-aramid with increased mechanical properties of the fibers.

Experimental

Materials

100 % meta-aramid plain fabrics were obtained from

*Corresponding author: dengjianguo88@outlook.com
*Corresponding author: genyang.cao@wtu.edu.cn
†These authors contribute equally to this work.

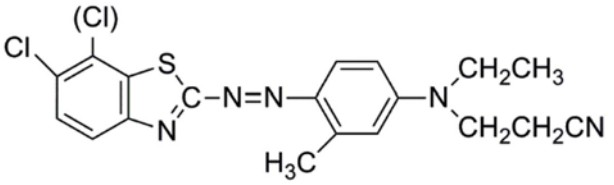

Figure 1. Chemical structure of the dye.

Shandong Taihe New Materials Co., Ltd., China. Disperse dye (C.I. Disperse Red 153) was purchased form Lonsen Company (China). The chemical structure of this dye is shown in Figure 1. N,N-dimethylacetamide (DMAc), ethanol, caustic soda, sodium hydrosulfite, and sodium alginate (analytically pure) were supplied by Sinopharm Chemical Reagent Co., Ltd. China. Penetrant JFC (industrial Pure) was supplied by Wuhan Hongxinkang Fine Chemical Co., Ltd., China.

Dyeing

The dye solution formulations were as follows: dye concentration is 10 g/*l*, sodium alginate concentration is 0.1 g/*l*, JFC concentration is 0.5 g/*l*. Seven DMAc concentrations, specifically, 0 %, 10 %, 30 %, 50 %, 70 %, 90 %, and 100 % (on bath volume) were used. All reagents and solvents were mixed for 30 min in the ultrasonic disperser (Kunshan Ultrasonic Instrument Co., Ltd., China). Then the meta-aramid fabric was soaked in a previously obtained dye solution for 5-10 min. The fabric was then taken out and applied for padding until the pick-up reached 200 %.

The dyeing process was carried out on a flat hot-pressing machine (Wuhan Qien Technology Co., Ltd., China) which was pre-heated to 200 °C with a pressure of 5 MPa for 10 min. After dyeing, all the dyed meta-aramid fabrics were rinsed by reduction cleaning using 4 g/*l* sodium hydrosulfite and 2 g/*l* sodium hydroxide at 80 °C for 20 min. Then the fabrics were washed using running water for 5 min, and then dried in an oven at 70 °C (Figure 2).

Measurements and Characterizations

The thermal stability of the fabric was carried out on the thermogravimetric analyzer (Sta409pc, NETZSCH Group, Germany). The temperature range was 25-800 °C, the heating rate was 10 °C/min, and the nitrogen flow rate was 20 m*l*/min.

The single-fiber strength tester (LLY-06E, Laizhou Electronic Instrument Co., Ltd., China) was used to test the single-fiber strength of the fiber. The spacing between fixtures was 10 mm. The tensile speed was 20 mm/min and the pre-tension was 0.2 cN. Measurements were repeated 100 times for each sample, and the results were averaged.

The crystal structure of the sample was analyzed using an X-ray diffractometer (D8 ADVANCE, Bruker-AXS, Germany). The X-ray used was a Cu-K_α ray with a wavelength of 0.154 nm and a scanning speed of 5 °/min. The scanning angle was varied from 0 ° to 40 °. The crystallinity of fiber was calculated using Jade 6.0 software according to the following equation [23].

$$x = \frac{\Sigma I_C}{\Sigma I_C + \Sigma I_a} \quad (1)$$

where ΣI_c is the total diffraction integral intensity of the crystalline portion and ΣI_a is the scattering integral intensity of the amorphous part.

The dispersion state of the dye in a solvent was observed by a transmission electron microscope (TEM) (JEM2100, Nippon Electronics Co., Ltd., Japan). 1 μ*l* solution was taken out by a pipette and dropped onto the copper mesh. After the copper mesh completely dried, it was loaded onto the liquid sample rod.

The field emission transmission electron microscope (Tecnai G2 F30, FEI Co., Ltd., USA) was used to scan the cross-section of the fiber. Before the test, the fiber was embedded in resin and cut into thin slices of 100 nm.

The *K/S* value of the fabric was measured on an X-Rite Color i7 colorimetric spectrophotometer (USA) spectrophotometer with a 10 ° standard observer and D65 illuminant. Five different points were measured for each sample and

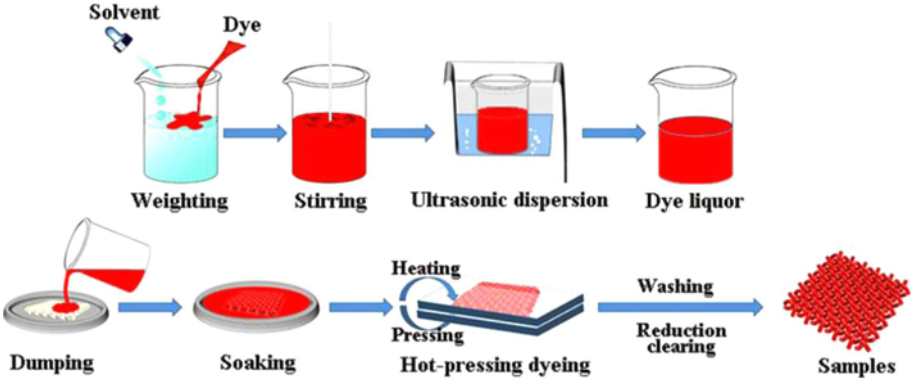

Figure 2. Dyeing process.

averaged.

Optical photos of the dyed fiber cross-section were taken by the Pannoramic MIDI digital section scanning and analysis system (3DHISTECH Ltd., Hungary). The fibers were embedded in resin and sliced. The thickness of each slice was 8 μm. The scanning speed was 1 cm^2/min.

The dry and wet fastness of the fabrics were carried out on the electric rubbing color fastness tester (G6345, Standard Group (Hong Kong) Co., Ltd., China) according to the National Standard GB/T 3920-2008, Color fastness to rubbing of textiles.

Water fastness of the fabrics was tested on a washing fastness tester (SW-12A, Changzhou Dahua Electronic Instrument Co., Ltd., China) according to the National Standard GB/T 3920-1997, Color fastness to water fastness test of textiles. Light fastness of all the dyed fabrics was evaluated on a light fastness meter (FY3600, Wenzhou Fangyuan Instrument Co., Ltd., China) according to the AATCC 16:2004 methods.

Particle Flow Dyeing Mechanism

The dyeing mechanism of particle flow dyeing was described in Figure 3. When the meta-aramid fabric is soaked in the prepared dyeing solution, the dyeing solution uniformly saturates the meta-aramid fabric. DMAc can slightly swell the surface of the meta-aramid fiber, which increases the contact position of the dye molecules with meta-aramid fibers. This will make it easy for the dye to get into the meta-aramid fiber.

In the hot-pressing dyeing process, under the high temperature, DMAc will vaporize and disperse dye will sublimate, the gaseous DMAc and disperse dye combine to form a single dye liquid particle, and numerous particles gather together to form a particle flow. The DMAc could protect the dye in the particle flow from oxidized by the oxygen in the air. Meanwhile, DMAc forms a muggy and semi-closed dyeing environment with the meta-aramid fabric. In this semi-closed damp-heat dyeing environment, DMAc particles carry disperse dye particles continuously collide the surface of the meta-aramid fiber. DMAc can destroy the hydrogen bonds between the macromolecules in the amorphous region of the meta-aramid fiber, and the pressure helps the disperse dye particles in the particle flow to quickly enter meta-aramid fibers for fast and efficient dyeing.

Results and Discussion

Effect of DMAc Hot-Pressing on Fiber Thermal Stability

Figure 4 shows the thermal weight loss curve of meta-aramid fiber before and after hot-pressing using DMAc. It can be seen that in the initial stage, the DTG curves of meta-aramid before and after hot-pressing showed significant drop near 70 °C. This is due to the presence of a certain

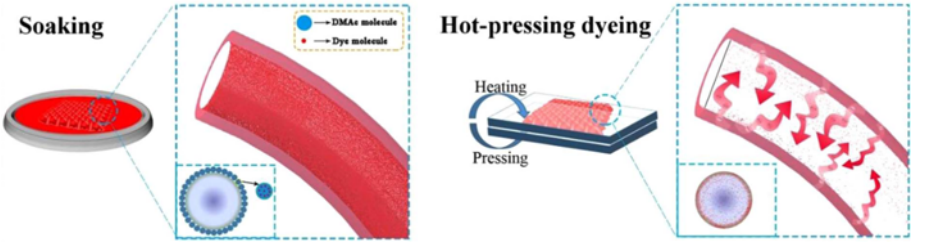

Figure 3. Particle flow dyeing mechanism.

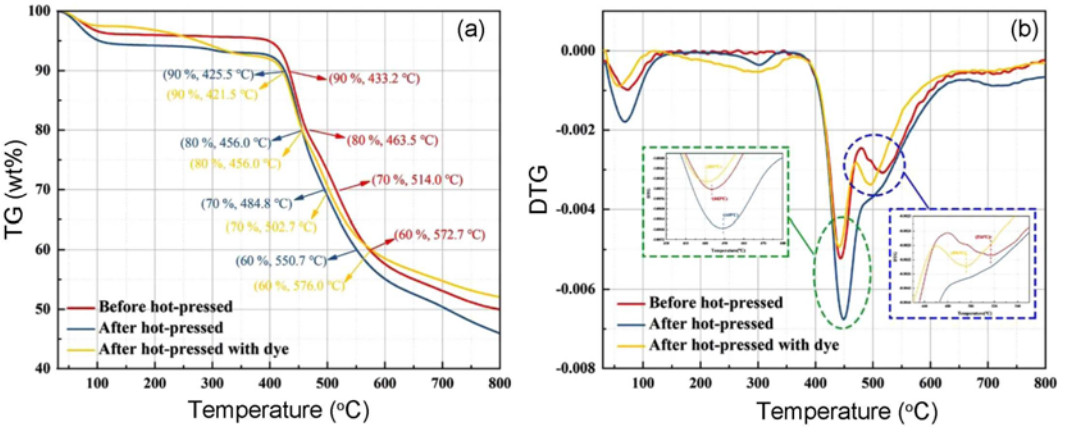

Figure 4. Thermogravimetric curves of meta-aramid fiber before and after hot-pressing with DMAc; (a) TG curve and (b) DTG curve.

Table 1. Thermal weight loss data of meta-aramid fiber before and after hot-pressing with DMAc

Sample	Initial stage		Carbonization decomposition			
	T (°C)	Weight loss (%)	*T* (°C)	Weight loss (%)	DTG maximum peak (°C)	DTG secondary peak (°C)
Before hot-pressed	30-352	4.4	353-659	40.4	443	516
After hot-pressed	30-353	7.0	354-659	40.9	449	-
After hot-pressed with dye	30-352	7.3	353-659	36.6	441	496

amount of water in the sample. This water includes both free water and the water adsorbed on the surface of the sample, which will cause a mass loss during the heating process.

After hot-pressed with DMAc, the meta-aramid showed a clear absorption peak at around 300 °C (which is absent in the meta-aramid before hot-pressing). This revealed that DMAc destroyed the hydrogen bonds between the fibers. Then the volatile matter bound on the surface of the fiber could leave the fabric during heating and form an absorption peak centered around 300 °C. The higher weight loss ratio of 7.0 % (Table 1) of meta-aramid after hot-pressing than that of meta-aramid before hot-pressing (4.4 %) also implied the breakage of hydrogen bonds after hot-pressing.

With increased temperature from 350 °C to 660 °C, all samples showed rapid decomposition by a significant decrease in the TG curve. This revealed a carbonization decomposition stage.

Table 1 showed the thermal weight loss data of the meta-aramid fiber before and after hot-pressing with DMAc. It can be seen that the differential thermal weight loss temperature of the meta-aramid after DMAc treatment is slightly higher than that of the original. This may be because DMAc caused the fiber swell and resulted in an increased free volume between fibers. Increased free volume facilitates the thermal motion of the molecular chains and allowed the rearranged of molecular chains on the surface of the fibers. Rearranged molecular chains lead to the improved thermal stability of the fibers.

Effect of DMAc Hot-Pressing on the Mechanical Properties of the Fiber

Table 2 shows the mechanical properties of the meta-aramid fiber before and after hot-pressing with DMAc. The mechanical properties of the meta-aramid fiber after hot-pressing with DMAc were improved by increasing the breaking strength and breaking elongation from 3.6 to 4.4 cN/dtex and 26.2 % to 28.3 %, respectively.

Table 2. Single fiber strength of meta-aramid fiber before and after hot-pressing with DMAc

Sample	Breaking strength (cN/dtex)	Breaking elongation (%)
Before hot-pressed	3.6±0.8	26.2±4.7
After hot-pressed	4.4±0.6	28.3±5.1
After hot-pressed with dye	4.7±0.6	29.3±5.1

As mentioned above, after rearrangement, more ordered the molecular chain orientation will form and thus improve both the crystallinity and mechanical stability of meta-aramid fibers.

Effect of DMAc Hot-Pressing on the Crystal Structure of the Fiber

Figure 5(a) shows the XRD pattern of the meta-aramid fiber before and after hot-pressing with DMAc. The spectrum showed that the diffraction peaks of the meta-aramid fibers appear at about $2\theta=17^{o}$, $2\theta=23^{o}$, and $2\theta=27^{o}$ [24-26]. These diffraction peaks of the meta-aramid fibers did not change significantly after hot-pressing with DMAc. DMAc hot-pressing had little effect on the crystal structure of the fiber which could be evidenced by the unchanged crystal structure before and after hot-pressing. Table 3 lists the crystallinity of the meta-aramid fiber before and after hot-pressing with DMAc. It can be seen that the crystallinity of the meta-aramid fiber after hot-pressing with DMAc increased from 44.6 % to 51.2 %. The degree of molecular chain freedom will increase due to the swelling effect of DMAc to meta-aramid. High temperature and high pressure during hot-pressing provide a driving force for the rearrangement of meta-aramid molecular chains. These high temperature and high pressure were also favorable for the crystallization and then enlarged the crystal region, resulting in an increased crystallinity.

Cross-sectional TEM images of meta-aramid fiber before and after hot-pressing with DMAc were given in Figure 5(b). Meta-aramid fiber after hot-pressing with DMAc showed a sheath-core structure. The unclear interface of the sheath-core for meta-aramid fiber before hot-pressing indicates a gradual transition trend. While meta-aramid fiber after hot-pressing with DMAc showed an interface between the sheath and core. Also, a clear boundary layer (Figure 5(b)) could be found in meta-aramid fiber after hot-pressed with DMAc. This layer indicated that DMAc entered the surface layer of the fiber and caused the swelling of the surface layer of the fiber. Thus, enlarged free volume between molecular chains facilitated the recrystallization of the amorphous phase under high temperature and high pressure. This recrystallization leads to an increase in the

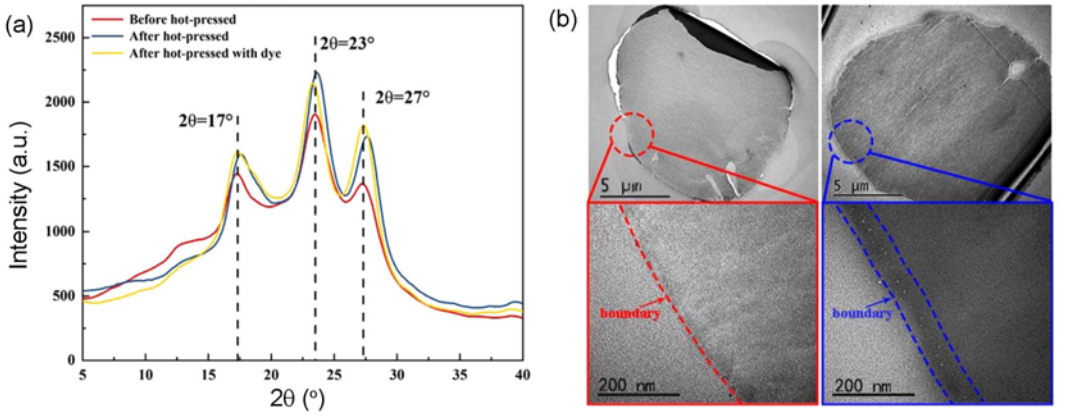

Figure 5. Effect of DMAc hot-pressing on the crystal structure of fiber; (a) XRD pattern of meta-aramid fiber before and after hot-pressing with DMAc and (b)TEM of the cross-section of meta-aramid fiber before and after hot-pressing with DMAc.

Table 3. Crystallinity of meta-aramid fiber before and after hot-pressing with DMAc

Sample	Crystallinity (%)
Before hot-pressed	44.6
After hot-pressed	51.2
After hot-pressed with dye	51.0

density of the boundary layer of the fiber, owing to which there is a significant color difference between the boundary layer of the fiber and the inside of the fiber. This density change was also consistent with increased crystallinity, and improved thermal and mechanical properties of the fiber.

Effect of DMAc Concentrations on the Dyeing Effect of Meta-Aramid

Figure 6(a, b) shows the dispersion state of the dye molecules in different solvents. The dispersion state of the dye molecules in water and DMAc was greatly different. The dispersion of dye molecules in water is not good, and considerable agglomeration occurs. While in DMAc, the dye molecules were uniformly dispersed and appeared as particles with a diameter of around 176 nm. This is because the high polarity of DMAc helps the dye molecules to be evenly distributed in the solvent.

Figure 6(c) shows the *K/S* values of the fibers after dyeing with different concentrations of DMAc. DMAc is a strong polar solvent that promotes the dye adsorption or swelling of aramid fibers [26]. When the concentration of DMAc is increased, the *K/S* value of the dyed meta-aramid increases, which is due to the increased swelling ability of DMAc along with increased DMAc concentrations. From Figure 6(b), one can observe that the dye can be well dispersed in DMAc. With increased DMAc concentration, the effects of DMAc on the meta-aramid and dye increases, which increasingly helps the dye to diffuse into the interior of the fiber, thereby increasing the dye uptake rate. This can be

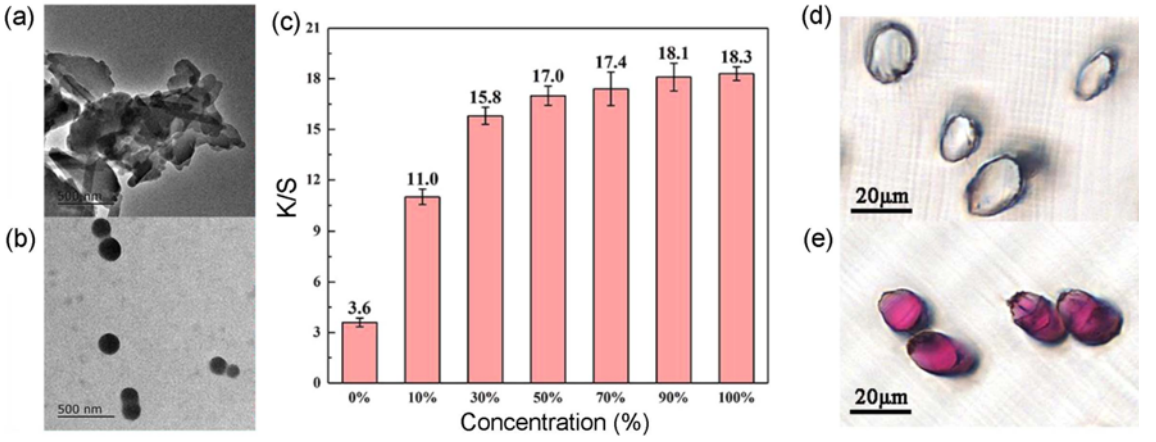

Figure 6. Effect of DMAc concentrations on the dyeing effect of meta-aramid; (a) the state of dye in water, (b) the state of dye in DMAc, (c) *K/S* value of fiber after hot-pressing dyeing with different concentration of DMAc, (d) fiber after hot-pressing dyeing with water, and (e) fiber after hot-pressing dyeing with DMAc.

Table 4. Color fastness of fibers after dyeing with different DMAc concentrations

Concentration	Rubbing fastness (dry/wet)	Washing fastness	Light fastness
0 %	1-2/2-3	3	1-2
10 %	1-2/2-3	2-3	2
30 %	1-2/3	2	2
50 %	2/3	3	2-3
70 %	2-3/3	3-4	2-3
90 %	3/3-4	3	3
100 %	3/3-4	3-4	3

seen intuitively in Figure 6(d) and (e). Without DMAc, the white core of the meta-aramid fiber indicated that the dye could not enter the fiber and just adhered to the fiber surface. After adding DMAc, the rose-red core of the fiber indicated that the dye diffused into the interior of the fiber thus achieved a much better dyeing effect. This meant that DMAc could promote the dyeing of meta-aramid fibers by increasing the diffusion of the dye in the fibers.

Table 4 lists the effect of DMAc concentrations on the color fastness of dyed fiber. The rubbing fastness and washing fastness of the dyed meta-aramid fabrics were heightened with increased DMAc concentration. When the concentration of DMAc exceeded 70 %, the dyed meta-aramid dyed fabric showed better color fastness. This may imply that 70 % DMAc is the lower limit to swell the meta-aramid fiber and to achieve a firm dye-fiber combination.

Conclusion

A combined dyeing method by integrating the advantages of both carrier dyeing and hot-pressing dyeing was utilized for the dyeing of meta-aramid. The mechanical properties and thermodynamic stability of the fiber after hot-pressing were both increased. XRD results showed increased corresponding fiber crystallinity. TEM showed that the disperse dyes were well dispersed in DMAc. Cross-sectional optical photographs of dyed fibers revealed that the dyes were successfully carried into the interior of the fiber under the synergic effect of temperature and pressure. Combined with hot-pressing dyeing, the dyeing cycle for the meta-aramid could be greatly shortened and the amounts of dyes and carriers could be significantly reduced.

Acknowledgments

This work was supported by the National Natural Science Foundation of China (Grant 51773158).

References

1. Z. Cheng, B. Li, J. Huang, T. Chen, Y. Liu, X. Wang, and X. Liu, *Mater. Des.*, **106**, 216 (2016).
2. S. Li, K. Han, H. Rong, X. Li, and M. Yu, *J. Appl. Polym. Sci.*, **131**, 40250 (2014).
3. C. X. Wang, M. Du, J. C. Lv, Q. Q. Zhou, Y. Ren, G. L. Liu, D. W. Gao, and L. M. Jin, *Appl. Surf. Sci.*, **349**, 333 (2015).
4. E. Tapie, V. P. W. Shim, and Y. B. Guo, *Int. J. Impact. Eng.*, **80**, 1 (2015).
5. N. Li, X.-K. Zhang, J.-R. Yu, Y. Wang, J. Zhu, and Z.-M. Hu, *Chin. J. Polym. Sci.*, **37**, 227 (2018).
6. F. Wang, Y. Wang, B. Hou, J. Zhang, and Y. Li, *Int. J. Adv. Manuf. Technol.*, **83**, 429 (2015).
7. H. Zheng and L. Zheng, *Fiber. Polym.*, **15**, 1627 (2014).
8. D. Sheng, Y. Wang, X. Wang, X. Lu, S. Jiang, H. Pan, G. Cao, and W. Xu, *Color. Technol.*, **133**, 320 (2017).
9. R. D. Kale, Y. Maurya, S. Dash, and T. Potdar, *Color. Technol.*, **134**, 464 (2018).
10. F. Azam, K. Iqbal, and F. Safdar, *Color. Res. Appl.*, **44**, 249 (2019).
11. G. Cao, D. Sheng, W. Xu, and X. Wang, *Color. Technol.*, **131**, 384 (2015).
12. M. R. Kim, H. Kim, and J. J. Lee, *Fiber. Polym.*, **14**, 2038 (2013).
13. E. M. Kim, B. G. Min, and J. Jang, *Fiber. Polym.*, **12**, 580 (2011).
14. Y. Dong and J. Jang, *Color. Technol.*, **127**, 173 (2011).
15. M. Trigo-López, Á. Miguel-Ortega, S. Vallejos, A. Muñoz, D. Izquierdo, Á. Colina, F. C. García, and J. M. García, *Dyes Pigm.*, **122**, 177 (2015).
16. M. T. Islam, F. Aimone, A. Ferri, and G. Rovero, *Dyes Pigm.*, **113**, 554 (2015).
17. H. D. Zheng, J. Zhang, J. Yan, and L. J. Zheng, *RSC Adv.*, **7**, 3470 (2017).
18. E. M. Kim and J. H. Choi, *Fiber. Polym.*, **12**, 484 (2011).
19. L. Y. Lei, Y. H. Mao, X. F. Xu, J. Q. Zheng, Q. K. Zheng, Y. Guan, and X. M. Fan, *Color. Technol.*, **130**, 349 (2014).
20. R. A. F. Moore and H. D. Weigmann, *Text. Res. J.*, **56**, 254 (1986).
21. A. P. Manian and J. N. Etters, *AATCC. Rev.*, **2**, 19 (2002).
22. S. Hussamy, *U.S. Patent*, US4836828A (1987).
23. Y. P. Zhu and X. Chen, *Research & Exploration in Laboratory*, **3**, 41 (2010).
24. C. Tang, X. Li, Z. Li, W. Tian, and Q. Zhou, *Polymers*, **10**, 1348 (2018).
25. H. Zheng, J. Zhang, B. Du, Q. Wei, and L. Zheng, *Fiber. Polym.*, **16**, 1134 (2015).
26. D. Sheng, B. Deng, G. Cao, B. Liu, H. Pan, S. Jiang, X. Chen, Y. Zhang, W. Gao, and W. Xu, *Dyes Pigm.*, **163**, 111 (2019).